

# Synchronization in discrete-time networks with general pairwise coupling

Published in Nonlinearity **22** (2009) 2333-2351.

Frank Bauer\*      Fatihcan M. Atay<sup>†</sup>      Jürgen Jost<sup>‡</sup>

Max Planck Institute for Mathematics in the Sciences  
Inselstrasse 22, D-04103 Leipzig, Germany

## Abstract

We consider complete synchronization of identical maps coupled through a general interaction function and in a general network topology where the edges may be directed and may carry both positive and negative weights. We define mixed transverse exponents and derive sufficient conditions for local complete synchronization. The general non-diffusive coupling scheme can lead to new synchronous behavior, in networks of identical units, that cannot be produced by single units in isolation. In particular, we show that synchronous chaos can emerge in networks of simple units. Conversely, in networks of chaotic units simple synchronous dynamics can emerge; that is, chaos can be suppressed through synchrony.

Mathematics Subject Classification: 05C50, 37D45, 37E05, 39A11

PACS numbers : 05.45.-a, 05.45.Ra, 05.45.Xt

## 1 Introduction

Synchronization in complex networks has been studied extensively by many scientists in the past years (for recent reviews see [1, 2, 3]). Specific application areas include social networks (opinion formation, finance, and world trade web), biological networks (genetic networks, cardiac rhythms, and neural networks), and technological networks (wireless communication networks and power-grids); see [1] and the references therein. Synchronization is one particular collective behavior in complex networks that emerges through the interaction of the constituent units. Complex systems are generally characterized by the richness of emergent behavior arising from the interaction of many elements or agents, which themselves are typically rather simple and often interact only locally or with only a few other ones. How dynamically rich behavior can emerge in a network of simple units is an important general question in complexity. In this article, we study the relation of

---

\*bauer@mis.mpg.de

<sup>†</sup>fatay@mis.mpg.de; <http://private-pages.mis.mpg.de/fatay>

<sup>‡</sup>jjost@mis.mpg.de

the concept of emergence to synchronization<sup>1</sup>, in the setting of coupled identical map networks.

Coupled map networks introduced by Kaneko [4] have become one of the standard models in synchronization studies. Particularly, chaotic synchronization can be investigated already in simple one-dimensional maps, which, as is well-known, would require at least three dimensions in the continuous-time case. On the one hand, a chaotic system's sensitive dependence to initial conditions would tend to lead the coupled system away from synchrony in the presence of ever-so-small perturbations. On the other hand, a diffusive coupling<sup>2</sup> between the units tends to equalize the states of neighboring units by providing a driving force that grows with the difference of the states, thereby driving the system towards synchrony. In the interplay between these two effects, it has indeed been discovered that diffusively coupled chaotic systems can exhibit robust synchronization for an appropriate range of parameters. Synchronization in diffusively-coupled map networks with positive weights is now well understood: One finds that the synchronizability of the network depends on the underlying network topology (given by the eigenvalues of the coupling matrix) and the dynamical behavior of the individual units (given by the largest Lyapunov exponent) [5, 6].

A notable aspect of diffusively coupled systems of identical units is that, while diffusive coupling tends to drive the network towards synchrony, the synchronized network shows exactly the same dynamical behavior as a single isolated unit. This is a simple consequence of the fact that the coupling term vanishes at the synchronized state. Hence, normally no new behavior arises through synchronization of diffusively-coupled systems. A notable exception is in the presence of time delays: It has been discovered that networks with time delays not only are able to synchronize (in fact sometimes better than undelayed networks), but also can exhibit a very rich range of new synchronized behavior [7, 8].

However, new synchronized behavior can not only be observed in diffusively coupled networks, when time-delays are present. In this work we show that also in non-diffusively coupled networks new synchronized behavior is emerging. The focus of this work is to understand, in detail, the impact of non-diffusive coupling schemes on the synchronized behavior. The synchronized behavior of a non-diffusively coupled network can be very different from the individual dynamics of its components (units). In contrast to diffusively-coupled networks, the overall coupling strength does not only determine the robustness of the synchronous state but also the emerging synchronous dynamics, i.e. by changing the overall coupling strength, different synchronous dynamics can be exhibited by the same system. In particular we shall see the following two extreme cases. Synchronized chaos can emerge in networks of simple units and chaos can be suppressed in a network of chaotic units.

## 2 General pairwise coupling

We consider a network of identical units that interact with each other. The coupling topology will affect the resulting dynamics in such a network. In many real world applications the connection structure is not bidirectional. Furthermore the influence of other units can be excitatory or inhibitory. These phenomena can, for example, be observed

---

<sup>1</sup>There exists several notions of synchronization [3]. In this work we study complete synchronization, where the differences between the states of coupled units tend to zero.

<sup>2</sup>Diffusive coupling refers to a coupling function that vanishes whenever its arguments are the same, see (2).

in neural networks, where there exists excitatory and inhibitory synapses and only the pre-synaptic neuron influences the post-synaptic one but not vice versa. Examples of synchronization in simple models of neural networks are investigated in [9]. Since different networks interact through different interaction functions, we want to keep our coupling function sufficiently general. Taking all these requirements into account, we study the following network model.

Let  $\Gamma$  be a non-trivial, weighted, directed graph on  $n$  vertices. The weight of the connection from vertex  $j$  to vertex  $i$  is denoted by  $w_{ij}$ , which could be positive, negative or zero. Positive and negative weights could model, for instance, excitatory and inhibitory connections, respectively. We assume that the network has no self-loops, that is,  $w_{ii} = 0$  for all  $i$ . The in-degree of vertex  $i$  is denoted by  $d_i = \sum_{j=1}^n w_{ij}$ . Even if a vertex is not isolated, it is possible that the in-degree of this vertex is equal to zero because of cancellations between positive and negative weights. These vertices are called quasi-isolated vertices, because their properties are very similar to isolated vertices [10]. Note that by definition every isolated vertex is quasi-isolated. In the following we will identify each unit with a vertex of a graph. This correspondence allows us to make use of graph theoretical methods.

The activity at vertex or unit  $i$  at time  $t + 1$  is given by:

$$x_i(t+1) = f(x_i(t)) + \epsilon \sigma_i \sum_{j=1}^n w_{ij} g(x_i(t), x_j(t)) \quad i = 1, \dots, n, \quad (1)$$

where

$$\sigma_i = \begin{cases} \frac{1}{d_i} & \text{if } d_i \neq 0 \\ 0 & \text{if } d_i = 0, \end{cases}$$

$f : \mathbb{R} \rightarrow \mathbb{R}$  and  $g : \mathbb{R}^2 \rightarrow \mathbb{R}$  are differentiable functions, and  $\epsilon \in \mathbb{R}$  is the overall coupling strength. In the following we assume that the derivatives of  $f$  and  $g$  are bounded along synchronous solutions  $s(t)$  of system (1), where all units exhibit the same behavior for all time i.e.,

$$x_i(t) = s(t) \quad \forall i, t.$$

The function  $f$  describes the dynamical behavior of the individual units whereas  $g$  characterizes the interactions between different pairs of units.

We say that the interaction is diffusive if the coupling function  $g$  satisfies the general diffusion condition

$$g(x, x) = 0 \quad \forall x \in \mathbb{R}. \quad (2)$$

A synchronous solution always exists if the interaction function  $g$  satisfies (2). Under this assumption the dynamical behavior of the whole network is exactly the same as the dynamical behavior of the isolated units, that is,

$$s(t+1) = f(s(t)). \quad (3)$$

However, if (2) is not satisfied then a synchronous solution may not always exist. Indeed, if  $s(t)$  is a synchronous solution such that  $g(s(t), s(t)) \neq 0$  for some  $t$ , then (1) implies that either  $\sigma_i = 0$  for all  $i$ , or  $\sigma_i \neq 0$  for all  $i$ . In other words, a synchronized solution exists only if all vertices are quasi-isolated or none of them are. The first case is trivial as there is no interaction. Therefore, for the study of emergent dynamics when (2) is not

satisfied, we shall later on restrict ourselves to the second case, i.e., to networks without quasi-isolated vertices. For such networks synchronous solutions exist and satisfy

$$s(t+1) = f(s(t)) + \epsilon g(s(t), s(t)). \quad (4)$$

Eq. (4) already shows that the synchronous behavior of the network is different from the behavior of isolated units. However, at this point it is not clear whether a synchronized state is robust against perturbations. We will study this issue in some detail in the following sections.

It is important to note that the interactions between the different units in Eq. (1) are “normalized” by the factor  $\sigma_i$ . Otherwise a synchronous solution would only exist, in the non-diffusive case, under the assumption that all vertices have the same vertex in-degree. Consequently a synchronous solution would only exist for regular graphs.

### 3 The coupling matrix

For diffusively coupled networks, the graph Laplacian is the natural coupling matrix. For a directed, weighted graph without loops, the (normalized) graph Laplacian  $\mathcal{L}$  is defined as,

$$(\mathcal{L})_{ij} := \begin{cases} 1 & \text{if } i = j \text{ and } d_i \neq 0. \\ -\frac{w_{ij}}{d_i} & \text{if there is a directed edge from } j \text{ to } i \text{ and } d_i \neq 0. \\ 0 & \text{otherwise.} \end{cases}$$

Here in the more general coupling case, the natural coupling matrix is given by  $\mathbf{K}$ , where  $\mathbf{K}$  for a directed, weighted network without loops, is defined as

$$(\mathbf{K})_{ij} := \begin{cases} 1 & \text{if } i = j \text{ and } d_i = 0. \\ \frac{w_{ij}}{d_i} & \text{if there is a directed edge from } j \text{ to } i \text{ and } d_i \neq 0. \\ 0 & \text{otherwise.} \end{cases}$$

Let the eigenvalues of  $\mathbf{K}$  and  $\mathcal{L}$  be labeled as  $\lambda_1, \dots, \lambda_n$  and  $\lambda'_1, \dots, \lambda'_n$ , respectively. Since the row sums of  $\mathbf{K}$  are equal to 1,  $\mathbf{K}$  has always an eigenvalue equal to 1, which corresponds to the eigenvector  $\mathbf{e} = (1, \dots, 1)^\top$ .

We briefly discuss the relationship between the coupling matrix  $\mathbf{K}$  and the graph Laplacian  $\mathcal{L}$  for directed weighted graphs. The graph Laplacian  $\mathcal{L}$  and the coupling matrix  $\mathbf{K}$  are related to each other by

$$\mathcal{L} = \mathbf{I} - \mathbf{K},$$

where  $\mathbf{I}$  is the  $n \times n$  identity matrix. Thus we have

$$\lambda'_i = 1 - \lambda_i, \quad \forall i. \quad (5)$$

Hence the multiplicity of the zero eigenvalue of  $\mathcal{L}$  is equal to the multiplicity of the eigenvalue  $\lambda = 1$  of  $\mathbf{K}$ .

The spectral properties of  $\mathcal{L}$  and  $\mathbf{K}$  for directed graphs with mixed signs are investigated systematically in [10]. The presence of directed edges or mixed signs leads to some interesting differences in the spectrum of  $\mathcal{L}$  compared to the case of undirected edges and nonnegative weights. For convenience of the reader, we mention here some of these differences. For undirected graphs with nonnegative weights it is well-known that

all eigenvalues of  $\mathcal{L}$  are real [11]. However, this is not true anymore if one studies directed graphs or mixed signs. Furthermore, while in the case of only nonnegative weights the absolute values of the eigenvalues are bounded by 2 [11], this is no longer true for the case of mixed signs. Indeed, using Gershgorin's Theorem [12] we have the following estimate.

**Lemma 1.** *Let  $\mathcal{D}(c, r)$  denote the disk in the complex plane centered at  $c$  and having radius  $r$ . Assume that there is at least one non quasi-isolated vertex (otherwise  $\mathcal{L}$  is equal to the zero matrix). Then all eigenvalues of the graph Laplacian  $\mathcal{L}$  are contained in the disk  $\mathcal{D}(1, r)$ , where*

$$r := \max_i \frac{\sum_{j=1}^n |w_{ij}|}{\left| \sum_{j=1}^n w_{ij} \right|} = \max_i \frac{\sum_{j=1}^n |w_{ij}|}{|d_i|}, \quad (6)$$

with the convention  $|d_i|^{-1} = 0$  if  $d_i = 0$ .

Note that the radius  $r$  in Eq. (6) can be written in the form

$$r = \max_i \left| \frac{d_i^+ + d_i^-}{d_i^+ - d_i^-} \right|,$$

where  $d_i^+ := \sum_{j: w_{ij} \geq 0} w_{ij}$  is the positive in-degree and  $d_i^- := \sum_{j: w_{ij} \leq 0} |w_{ij}|$  the negative in-degree. So, for fixed sum  $d_i^+ + d_i^-$ , the closer  $d_i^+$  and  $d_i^-$  are, the larger is the radius  $r$ . Clearly,  $r = 1$  when the weights are nonnegative, but  $r$  can be much larger in the case of signed weights. The radius  $r$  will play an important role in Chapter 6 where we derive sufficient conditions for synchronization.

Since we deal with a graph  $\Gamma$  with both positive and negative weights, we should make some notions precise. Let the weighted adjacency matrix of  $\Gamma$  be given by  $\mathbf{W} = [w_{ij}]$ . Define the corresponding (usual) graph  $\Gamma'$  with adjacency matrix  $\mathbf{A} = [a_{ij}]$  such that  $a_{ij} = 1$  if  $w_{ij} \neq 0$  and  $a_{ij} = 0$  otherwise. Then we say that  $\Gamma$  is strongly connected (resp. has a spanning tree) if  $\Gamma'$  is strongly connected (resp. has a spanning tree). In the general setting of directed edges and mixed signs, a non-complete graph refers to a graph where there exists at least one pair of distinct vertices with no link between them.

The multiplicity of the zero eigenvalue of  $\mathcal{L}$  can be bounded from below by the following two graph properties:

**Lemma 2.** *Let  $m_0$  be the multiplicity of the zero eigenvalue of  $\mathcal{L}$ .*

1. *If  $n_1$  denotes the number of quasi-isolated vertices, then*

$$n_1 \leq m_0.$$

2. *If  $n_2$  denotes the minimum number of trees needed to span the graph, then*

$$n_2 \leq m_0.$$

*Proof.* 1. Assume that there exists  $n_1$  quasi-isolated vertices in the graph. Then, there exists  $n_1$  rows of  $\mathcal{L}$  that consist entirely of zeros. Consequently,  $\mathcal{L}$  has at least  $n_1$  eigenvalues equal to zero.

2. Assume that one needs at least  $n_2$  trees to span the whole graph. Let  $\mathcal{L}$  be given

in Frobenius normal form [13], i.e. after possibly relabeling the vertices,  $\mathcal{L}$  is given in the form

$$\mathcal{L} = \begin{pmatrix} \mathcal{L}_1 & \mathcal{L}_{12} & \dots & \mathcal{L}_{1p} \\ 0 & \mathcal{L}_2 & \dots & \mathcal{L}_{2p} \\ \vdots & \vdots & \ddots & \vdots \\ 0 & 0 & \dots & \mathcal{L}_p \end{pmatrix}, \quad (7)$$

where the block diagonal matrices  $\mathcal{L}_i$  correspond to the strongly connected components of the graph. The spectrum of  $\mathcal{L}$  then satisfies

$$\text{spec}(\mathcal{L}) = \bigcup_{i=1}^p \text{spec}(\mathcal{L}_i). \quad (8)$$

Since one needs  $n_2$  trees to span the whole graph, there exist  $n_2$  block matrices  $\mathcal{L}_i$  such that  $\mathcal{L}_{ij}$  is the zero matrix for  $i < j \leq p$ . Thus, these  $n_2$  block matrices  $\mathcal{L}_i$  have zero row sums because  $\mathcal{L}$  has zero row sums. The result now follows from (8).  $\square$

## 4 Synchronization

We want to study synchronous solutions of Eq. (1) and whether the synchronous state is robust to perturbations. We say the system (1) (locally) synchronizes if

$$\lim_{t \rightarrow \infty} |x_i(t) - x_j(t)| = 0 \quad \forall i, j,$$

whenever the initial conditions belong to some appropriate open set<sup>3</sup>. In this article the term synchronization always refers to this definition.

### 4.1 General pairwise coupling and only quasi-isolated vertices

This case is not very insightful, as Eq. (1) implies that there are no interactions between the different units. The time evolution of each unit is given by Eq. (3). Thus the network only synchronizes if nearby orbits of the function  $f$  converge, i.e. the Lyapunov exponent

$$\mu_f := \overline{\lim}_{T \rightarrow \infty} \frac{1}{T} \sum_{s=\bar{t}}^{\bar{t}+T-1} \log |f'(s(t))|, \quad (9)$$

of  $f$  is negative. Here  $\bar{t}$  is chosen such that  $f'(s(t)) \neq 0$  for all  $t > \bar{t}$ . A negative Lyapunov exponent implies that the trajectory  $s(t)$  is already attracting for  $f$ , and hence, no emergence of new dynamics. Hence chaotic synchronization is not possible as chaos requires a positive Lyapunov exponent  $\mu_f$ .

### 4.2 General pairwise coupling without quasi-isolated vertices

To characterize this case we start with the following definition.

---

<sup>3</sup>If one considers chaotic synchronization, i.e.  $f + \epsilon g$  is chaotic, then there exists subtleties concerning this open set and the exact notion of attraction. These issues are carefully studied in [14]. For the purposes of this article, these subtleties are not important.

**Definition 3.** The  $k$ -th mixed transverse exponent  $\chi_k$  is defined for  $2 \leq k \leq n$  as:

$$\chi_k := \overline{\lim}_{T \rightarrow \infty} \frac{1}{T} \sum_{s=\bar{t}}^{\bar{t}+T-1} \log |h_k(s(t))|, \quad (10)$$

where

$$h_k(s(t)) = f'(s(t)) + \epsilon \partial_1 g(s(t), s(t)) + \epsilon \partial_2 g(s(t), s(t)) \lambda_k$$

and  $\bar{t}$  is chosen such that  $h(s(t)) \neq 0$  for all  $t > \bar{t}$ . If no such  $\bar{t}$  exists we set  $\chi_k = -\infty$ .

These exponents combine the dynamical behavior of the functions  $f$  and  $g$  with the network topology. Furthermore we define the *maximal mixed transverse exponent*  $\chi$  as

$$\chi := \max_{k \geq 2} \chi_k.$$

The next theorem shows that the maximal mixed transverse exponent governs the synchronizability of the network.

**Theorem 4.** System (1) synchronizes if the maximal mixed transverse exponent is negative.

Before we prove this theorem we prove the following theorem that also holds for time-dependent functions.

**Theorem 5.** Consider the system of equations

$$v_i(t+1) = \begin{cases} k_1(t)v_i(t), & i = 1, \\ k_1(t)v_i(t) + k_2(t)v_{i-1}(t), & i = 2, \dots, m, \end{cases} \quad (11)$$

where  $v_i \in \mathbb{R}$  and  $k_1$  and  $k_2$  are bounded functions on  $\mathbb{R}$ . Suppose there exists  $\bar{t} \in \mathbb{R}$  such that

$$k_1(t) \neq 0 \text{ for } t \geq \bar{t}. \quad (12)$$

Suppose further that

$$\eta := \overline{\lim}_{T \rightarrow \infty} \frac{1}{T} \sup_{t_0 \geq \bar{t}} \sum_{s=t_0}^{t_0+T-1} \log |k_1(s)| < 0. \quad (13)$$

Then for any  $\varepsilon \in (0, -\eta)$  there exists  $K_\varepsilon \geq 0$  such that all solutions of (11) satisfy

$$\|(v_1(t), \dots, v_m(t))\| \leq K_\varepsilon e^{(\eta+\varepsilon)(t-t_0)} \|(v_1(t_0), \dots, v_m(t_0))\| \quad (14)$$

for all  $t \geq t_0 \geq \bar{t}$ . On the other hand, if there is no such  $\bar{t}$  satisfying (12), then

$$\|(v_1(t), \dots, v_m(t))\| = 0 \text{ for all large } t. \quad (15)$$

*Proof.* The homogeneous equation

$$v_1(t+1) = k_1(t)v_1(t) \quad (16)$$

has the solution  $v_1(t) = \Phi(t, t_0)v_1(t_0)$ , where the state transition function  $\Phi$  is given by  $\Phi(t, t_0) = \prod_{s=t_0}^{t-1} k_1(s)$ ,  $t > t_0$ , and  $\Phi(t, t) = 1$  for  $\forall t$ . In the following,  $t_0 \geq \bar{t}$ . By (13), for any  $\varepsilon \in (0, -\eta)$  there exists  $T'$  such that

$$\sup_{t_0 \geq \bar{t}} \frac{1}{T} \sum_{s=t_0}^{t_0+T-1} \log |k_1(s)| < \eta + \frac{\varepsilon}{m} < 0, \quad \text{for all } T > T'.$$

Thus,

$$\prod_{s=t_0}^{t-1} |k_1(s)| \leq e^{(\eta + \frac{1}{m}\varepsilon)(t-t_0)}, \quad \text{if } t > t_0 + T',$$

whereas

$$\prod_{s=t_0}^{t-1} |k_1(s)| \leq M^{(t-t_0)} \leq M^{T'}, \quad \text{if } t_0 < t \leq t_0 + T'$$

where  $M = \sup_{t \in \mathbb{R}} |k_1(t)|$ . Thus,

$$\prod_{s=t_0}^{t-1} |k_1(s)| \leq C_1^\varepsilon e^{(\eta + \frac{1}{m}\varepsilon)(t-t_0)}, \quad \forall t > t_0 \geq \bar{t}$$

where the constant  $C_1^\varepsilon \geq \max\{M^{T'} e^{-(\eta + \frac{1}{m}\varepsilon)T'}, 1\}$  is independent of  $t_0$ . Consequently,

$$|\Phi(t, t_0)| \leq C_1^\varepsilon e^{(t-t_0)(\eta + \frac{1}{m}\varepsilon)}, \quad \forall t > t_0 \geq \bar{t}, \quad (17)$$

and the solution of the first equation in (11) satisfies

$$|v_1(t)| \leq C_1^\varepsilon e^{(\eta + \frac{1}{m}\varepsilon)(t-t_0)} |v_1(t_0)|. \quad (18)$$

Now the solution to (11) for  $i = 2, \dots, m$  is

$$v_i(t) = \Phi(t, t_0)v_i(t_0) + \sum_{s=t_0}^{t-1} \Phi(t, s+1)k_2(s)v_{i-1}(s). \quad (19)$$

Using (17) and (18) we estimate,

$$\begin{aligned} |v_2(t)| &\leq C_1^\varepsilon e^{(\eta + \frac{1}{m}\varepsilon)(t-t_0)} |v_2(t_0)| + C_1^\varepsilon \overline{k_2} \sum_{s=t_0}^{t-1} e^{(\eta + \frac{1}{m}\varepsilon)(t-s-1)} e^{(\eta + \frac{1}{m}\varepsilon)(s-t_0)} |v_1(t_0)| \\ &= C_1^\varepsilon e^{(\eta + \frac{1}{m}\varepsilon)(t-t_0)} |v_2(t_0)| + C_1^\varepsilon \overline{k_2} e^{(\eta + \frac{1}{m}\varepsilon)(t-t_0)} e^{-(\eta + \frac{1}{m}\varepsilon)(t-t_0)} |v_1(t_0)|, \end{aligned}$$

where  $\overline{k_2} = \sup_t |k_2(t)|$ . Adding to (18) yields

$$|v_2(t)| + |v_1(t)| \leq C_1^\varepsilon e^{(\eta + \frac{1}{m}\varepsilon)(t-t_0)} |v_2(t_0)| + C_1^\varepsilon e^{(\eta + \frac{1}{m}\varepsilon)(t-t_0)} (\overline{k_2} e^{-(\eta + \frac{1}{m}\varepsilon)(t-t_0)} + 1) |v_1(t_0)|.$$

Since there exists some constant  $C_2$  (we drop the dependence on  $\varepsilon$  for ease of notation) such that

$$C_1^\varepsilon e^{(\eta + \frac{1}{m}\varepsilon)(t-t_0)} (\overline{k_2} e^{-(\eta + \frac{1}{m}\varepsilon)(t-t_0)} + 1) \leq C_2 e^{(\eta + \frac{2}{m}\varepsilon)(t-t_0)}, \quad \forall t > t_0,$$

we have

$$|v_1(t)| + |v_2(t)| \leq C_2 e^{(\eta + \frac{2}{m}\varepsilon)(t-t_0)} (|v_1(t_0)| + |v_2(t_0)|), \quad \forall t > t_0 \geq \bar{t}. \quad (20)$$



For  $i = 3$ , the argument is similar with some slight modifications: We use the estimate from (17) as

$$|\Phi(t, t_0)| \leq C_1 e^{(t-t_0)(\eta + \frac{1}{m}\varepsilon)} \leq C_1 e^{(t-t_0)(\eta + \frac{2}{m}\varepsilon)}$$

in (19), while bounding  $|v_2(t)|$  by the right hand side of (20). Thus,

$$|v_3(t)| \leq C_1 e^{(\eta + \frac{2}{m}\varepsilon)(t-t_0)} |v_3(t_0)| + C_2 \sum_{s=t_0}^{t-1} e^{(\eta + \frac{2}{m}\varepsilon)(t-s-1)} \overline{k_2} e^{(\eta + \frac{2}{m}\varepsilon)(s-t_0)} (|v_1(t_0)| + |v_2(t_0)|).$$

Adding to (20) gives

$$\sum_{i=1}^3 |v_i(t)| \leq C_3 e^{(\eta + \frac{3}{m}\varepsilon)(t-t_0)} \sum_{i=1}^3 |v_i(t_0)|$$

for some constant  $C_3$ . Repeating for  $i = 4, \dots, m$ , we finally obtain

$$\sum_{i=1}^m |v_i(t)| \leq C_m e^{(\eta + \frac{m}{m}\varepsilon)(t-t_0)} \sum_{i=1}^m |v_i(t_0)|$$

which establishes (14) for the  $\ell_1$ -norm, and thus for all norms in  $\mathbb{R}^m$  for an appropriate constant  $K_\varepsilon$ .

To prove the last statement of the theorem, notice that if (12) fails for all  $t$ , then there exist an infinite sequence  $t_1 < t_2 < \dots$  of zeros of  $k_1$ . In this case, the equations (11) imply that  $v_i(t) = 0$  for all  $t \geq t_i + 1$ , yielding (15). This completes the proof.  $\square$

Now we prove Theorem 4.

*Proof of Theorem 4.* For general pairwise coupling and networks without quasi-isolated vertices, Eq. (1) can be written in the following form using the coupling matrix  $\mathbf{K}$

$$x_i(t+1) = f(x_i(t)) + \epsilon (\mathbf{K} \mathbf{g}(\mathbf{x}_i(t), \mathbf{x}(t)))_i, \quad (21)$$

where the vector  $\mathbf{g}(\mathbf{x}_i, \mathbf{x}) \in \mathbb{R}^n$  is defined as  $\mathbf{g}(\mathbf{x}_i, \mathbf{x}) := (g(x_i, x_1), \dots, g(x_i, x_n))^\top$  and  $(\mathbf{K} \mathbf{g}(\mathbf{x}_i(t), \mathbf{x}(t)))_i$  is the  $i$ th component of the vector  $\mathbf{K} \mathbf{g}(\mathbf{x}_i(t), \mathbf{x}(t))$ .

Let  $\mathbf{x}(t) = (x_1(t), \dots, x_n(t))$  and  $\mathbf{s}(t) = (s(t), \dots, s(t))$ . Small perturbations  $\mathbf{u}(t) = \mathbf{x}(t) - \mathbf{s}(t)$  of the synchronous state are governed by the variational equation

$$\mathbf{u}(t+1) = [f'(s(t)) + \epsilon \partial_1 g(s(t), s(t))] \mathbf{u}(t) + \epsilon \partial_2 g(s(t), s(t)) \mathbf{K} \mathbf{u}(t), \quad (22)$$

where  $\partial_i g$  denotes the  $i$ th partial derivative of  $g$ .

In the sequel we study the coupling matrix  $\mathbf{K}$  in Jordan form. There exists a non-singular matrix  $\mathbf{P}$  such that  $\mathbf{K} = \mathbf{P} \mathbf{J} \mathbf{P}^{-1}$  and  $\mathbf{J}$  is of the form

$$\mathbf{J} = \begin{pmatrix} \mathbf{J}_1 & & & \\ & \mathbf{J}_2 & & \\ & & \ddots & \\ & & & \mathbf{J}_m \end{pmatrix}. \quad (23)$$

Each Jordan block  $\mathbf{J}_l$  is of the form

$$\mathbf{J}_l = \begin{pmatrix} \lambda_l & 1 & & \\ & \ddots & \ddots & \\ & & 1 & \\ & & & \lambda_l \end{pmatrix} \in \mathbb{R}^{m_l \times m_l}, \quad (24)$$

where  $m_l$  is the block size of the Jordan block  $J_l$ . Without loss of generality we assume that  $\mathbf{J}_1$  corresponds to the eigenvalue  $\lambda_1 = 1$  with eigenvector  $\mathbf{e} := (1, \dots, 1)^\top$ . After the coordinate transformation,  $\mathbf{u}(t) \rightarrow \mathbf{P}^{-1}\mathbf{u}(t) =: \mathbf{v}(t)$ , Eq. (22) becomes:

$$\mathbf{v}(t+1) = [f'(s(t)) + \epsilon \partial_1 g(s(t), s(t))] \mathbf{v}(t) + \epsilon \partial_2 g(s(t), s(t)) \mathbf{J} \mathbf{v}(t). \quad (25)$$

For each Jordan-block  $\mathbf{J}_l$  this reads in component form:

$$v_i(t+1) = \begin{cases} h_l(s(t))v_i(t) + \epsilon \partial_2 g(s(t), s(t))v_{i+1}(t) & i = 1, \dots, m_l - 1 \\ h_l(s(t))v_i(t) & i = m_l \end{cases} \quad (26)$$

This is exactly of the form (11) with  $k_1 = h_l$  and  $k_2 = \epsilon \partial_2 g$ . We now apply theorem 5, noting that the time dependance in (26) arises from a trajectory of a time-invariant system, so choices of initial times are arbitrary. Thus, the perturbations decay for all Jordan blocks  $\mathbf{J}_i$ ,  $i = 2, \dots, m$ . For the Jordan block  $\mathbf{J}_1$  the situation is different because we do not assume that the mixed longitudinal exponent  $\chi_1$  (similarly defined as the mixed transverse exponents  $\chi_k$  in (10) for the eigenvalue  $\lambda_1 = 1$ ) is negative. Thus,  $v_1(t)$  does not have to decay. However, we are mainly interested in the behavior of the original perturbations  $\mathbf{u}(t) = \mathbf{P}\mathbf{v}(t)$ . Since  $\lambda_1 = 1$  corresponds to the eigenvector  $\mathbf{e} := (1, \dots, 1)^\top$  it is possible to choose  $\mathbf{P}$  such that

$$\mathbf{P} = \begin{pmatrix} 1 & p_{12} & \dots & p_{1n} \\ 1 & p_{22} & \dots & p_{2n} \\ \vdots & \vdots & & \vdots \\ 1 & p_{n2} & \dots & p_{nn} \end{pmatrix}. \quad (27)$$

Thus,  $\mathbf{u}(t) = \mathbf{P}\mathbf{v}(t)$  is given by

$$\mathbf{u}(t) = v_1(t)\mathbf{e} + \begin{pmatrix} \sum_{j=2}^n p_{1j}v_j(t) \\ \vdots \\ \sum_{j=2}^n p_{nj}v_j(t) \end{pmatrix}.$$

Since all the  $v_i(t)$ ,  $i = 2, \dots, n$  are decaying we conclude that

$$\begin{aligned} \lim_{t \rightarrow \infty} |x_i(t) - x_j(t)| &= \lim_{t \rightarrow \infty} |s(t) + u_i(t) - (s(t) + u_j(t))| \\ &= \lim_{t \rightarrow \infty} \left| s(t) + v_1(t) + \sum_{k=2}^n p_{ik}v_k(t) - \left( s(t) + v_1(t) + \sum_{k=2}^n p_{jk}v_k(t) \right) \right| \\ &= \lim_{t \rightarrow \infty} \left| \sum_{k=2}^n p_{ik}v_k(t) - \sum_{k=2}^n p_{jk}v_k(t) \right| = 0 \quad \forall i, j. \end{aligned}$$

□

**Remarks 6.**

- If in addition  $\chi_1 < 0$  then  $v_1(t)$  is also decaying. Thus the synchronous solution is attracting. Examples of attracting synchronous solutions are studied in Chapter 6.
- Theorem 4 can also be formulated in terms of the eigenvalues of the graph Laplacian  $\mathcal{L}$ . In this case one only has to replace  $\lambda_k$  by  $1 - \lambda'_k$ , according to equation (5).

In the following we study some special cases of coupling functions that appear commonly in applications.

### 4.3 Diffusive coupling with both quasi-isolated and non quasi-isolated vertices

For diffusive coupling a synchronous solution always exists. So, here we may permit the coexistence of both non-quasi-isolated and quasi-isolated vertices in the network. The general diffusion condition (2) implies that  $\partial_1 g(s(t), s(t)) = -\partial_2 g(s(t), s(t))$ . Because this leads to a cancellation of the artificially introduced term in the coupling matrix  $\mathbf{K}$  (1 when  $i = j$  and  $d_i = 0$ ), it follows that, even when there are non-quasi-isolated and quasi-isolated vertices in the graph, small perturbations  $\mathbf{u}(t) = \mathbf{x}(t) - \mathbf{s}(t)$  are governed again by the variational equation (22), and the same arguments apply as in section 4.2. In this case the  $k$ -th mixed transverse exponent for diffusively coupled units is given by

$$\chi_k^{\text{diff}} := \overline{\lim}_{T \rightarrow \infty} \frac{1}{T} \sum_{s=\bar{t}}^{\bar{t}+T-1} \log |h_k^{\text{diff}}(s(t))| \quad (28)$$

where

$$h_k^{\text{diff}}(s(t)) = f'(s(t)) + \epsilon \partial_2 g(s(t), s(t))(\lambda_k - 1)$$

and  $\bar{t}$  is chosen such that  $h(s(t)) \neq 0$  for all  $t > \bar{t}$ . If no such  $\bar{t}$  exists we set  $\chi_k^{\text{diff}} = -\infty$ .

For diffusive coupling, Theorem 4 implies that system (1) synchronizes if the maximal transverse exponent satisfies

$$\chi^{\text{diff}} := \max_{k \geq 2} \chi_k^{\text{diff}} < 0. \quad (29)$$

**Proposition 7.** Assume that the function  $f$  is chaotic, i.e. has a positive Lyapunov-exponent  $\mu_f$ . If

- there exists more than one quasi-isolated vertex

or

- the network does not possess a spanning tree

then the maximal mixed transverse exponent is positive.

*Proof.* If one of these conditions is fulfilled then by Lemma 2 the multiplicity of the zero eigenvalue satisfies  $m_0(\mathcal{L}) \geq 2$  and hence the multiplicity of the eigenvalue 1 of  $\mathbf{K}$  satisfies  $m_1(\mathbf{K}) \geq 2$ . Consequently,  $\chi_k^{\text{diff}} = \mu_f > 0$  for  $k = 2, \dots, m_0$ .  $\square$

In fact, it is intuitively clear that the presence of more than one quasi-isolated vertex or the absence of a spanning tree will in general make chaotic synchronization impossible, because in those situations, there will exist pairs of vertices none of which can dynamically influence the other. Note, however, that Proposition 7 does not exclude the so-called Master-Slave configurations.

A particular coupling function that arises in coupled map lattice models [15] is

$$g(x_i, x_j) = b(f(x_j) - f(x_i)) \quad (30)$$

where  $b$  is some real constant. In this case it is possible to separate the effects of the synchronous dynamics  $f$  and the network topology:

**Corollary 8.** *System (1) with the coupling function (30) synchronizes if*

$$\mu_f + \max_{k \geq 2} \log |1 + \epsilon b(\lambda_k - 1)| < 0. \quad (31)$$

This result was already obtained in undirected [5] and directed [6] networks, in both cases with nonnegative weights.

Assume that the synchronous solution  $f$  is chaotic, i.e.  $\mu_f > 0$ . Then the network topology term in (31) has to be sufficiently negative to compensate the positive Lyapunov exponent  $\mu_f$ . This in turn requires that the eigenvalues  $\lambda_k$  for  $k \geq 2$  be bounded away from one, and the coupling strength  $\epsilon$  lie in an appropriate interval.

#### 4.4 Direct coupling and only non-quasi-isolated vertices

Another important special case of the general coupling function  $g(x, x)$  is the so-called direct coupling<sup>4</sup>, where the interactions depend only on the state of the neighboring units, i.e.

$$g(x_i, x_j) = \hat{g}(x_j) \quad (32)$$

for some  $\hat{g} : \mathbb{R} \rightarrow \mathbb{R}$ . Thus  $\partial_1 g(s(t), s(t)) = 0$ , and the  $k$ -th mixed transverse exponent for directly coupled units is given by

$$\chi_k^{\text{direct}} := \overline{\lim}_{T \rightarrow \infty} \frac{1}{T} \sum_{s=\bar{t}}^{\bar{t}+T-1} \log |h_k^{\text{direct}}(s(t))| \quad (33)$$

where

$$h_k^{\text{direct}}(s(t)) = f'(s(t)) + \epsilon \hat{g}'(s(t)) \lambda_k.$$

and  $\bar{t}$  is chosen such that  $h(s(t)) \neq 0$  for all  $t > \bar{t}$ . If no such  $\bar{t}$  exists we set  $\chi_k^{\text{diff}} = -\infty$ . For direct coupling, Theorem 4 implies that system (1) synchronizes if the maximal mixed transverse exponent satisfies

$$\chi^{\text{direct}} := \max_{k \geq 2} \chi_k^{\text{direct}} < 0. \quad (34)$$

**Proposition 9.** *Assume that  $f + \epsilon \hat{g}$  is chaotic, i.e has a positive Lyapunov-exponent  $\mu_{(f+\epsilon \hat{g})}$ . If the network does not possess a spanning tree then maximal mixed transverse exponent  $\chi^{\text{direct}}$  is positive.*

---

<sup>4</sup>We borrow this term from [16].

*Proof.* Similar to the proof of Proposition 7.  $\square$

If in addition  $\hat{g}(x) = bf(x)$ , it is again possible to separate the effects of the resulting synchronized dynamics  $(1 + \epsilon b)f$  and the network topology.

**Corollary 10.** *Suppose that  $\hat{g}(x) = bf(x)$ . System (1) synchronizes if*

$$\max_{k \geq 2} \log \left| \frac{1 + \epsilon b \lambda_k}{1 + \epsilon b} \right| + \mu_{(1+\epsilon b)f} < 0. \quad (35)$$

Similar to the case of diffusively coupled units, if the resulting synchronous solution  $(1 + \epsilon b)f$  is chaotic, then the eigenvalues  $\lambda_k$  should be bounded away from one, and the coupling strength  $\epsilon$  lie in an appropriate interval.

## 5 Emergence of synchronized chaos in directly coupled networks

As mentioned in the introduction, in diffusively-coupled units, the synchronized network behaves exactly as a single unit would do in isolation. Hence, no new collective behavior is gained from synchronization: Either the units are dynamically complex, then so is the whole network, - or the units are dynamically simple then the behavior of the whole network will remain simple.

Eq. (4) shows that the requirement for new emerging collective behavior is that the general diffusion condition Eq. (2) is not satisfied. In this way, the network can display new behavior that the single isolated units are not capable to show. In particular we shall see in this section that synchronous chaos can emerge in a network of simple units.

One task in showing that simple units can exhibit synchronized chaos is to rigorously show that the synchronized solution is indeed chaotic. To this end, we consider S-unimodal maps.

### 5.1 A full family of S-unimodal maps

In general it is hard to prove that a function is chaotic. However there is one well-understood class of chaotic functions, namely the so-called full families of S-unimodal maps [17]. For convenience, we recall the notion of a full family of S-unimodal maps in the Appendix A.

#### Properties of full families of S-unimodal maps:

It is well-known that a full family of S-unimodal maps undergoes a sequence of period doubling bifurcations as  $\mu$  varies from  $\mu_0$  to  $\mu_1$  and finally becomes chaotic [17, 18].

As the main result of this section, we present a full family of S-unimodal maps.

**Theorem 11.** *Consider the family  $f_\mu$  of maps*

$$f_\mu(x) = \left( \frac{1 - e^{-\mu}}{1 + e^{-\mu}} x + 1 - \frac{2}{1 + e^{-\mu x}} \right) \Theta, \quad (36)$$

where  $\Theta < 0$ . This family is a full family of S-unimodal maps on  $[0, 1]$  with  $\mu \in [\mu_0 = 0, \mu_1]$  where we choose  $\mu_1$  such that  $f_{\mu_1}(c) = 1$ .

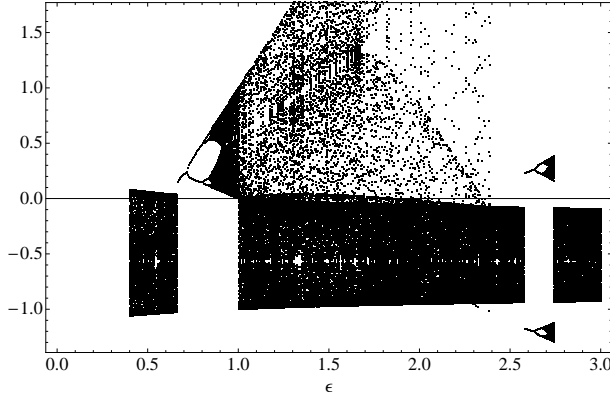


Figure 1: Bifurcation diagram for Eq. (36) with parameter values  $\Theta = -1.3041$  and  $\mu = 20$ .

The proof is given in Appendix B.

We can use the full family of S-unimodal maps (36) to demonstrate that synchronous chaotic behavior can emerge in a network of simple units. Let the individual dynamics be given by  $f(x) = \left(\frac{1-e^{-\mu}}{1+e^{-\mu}}x + 1\right)\Theta$  and the interaction between units by  $\hat{g}(x) = -\frac{2\Theta}{1+e^{-\mu x}}$ . Clearly, the individual dynamics are very simple, as  $f(x)$  has one single attracting fixed point. The resulting synchronous solution is

$$s(t+1) = \left(\frac{1-e^{-\mu}}{1+e^{-\mu}}s(t) + 1\right)\Theta - \frac{2\epsilon\Theta}{1+e^{-\mu s(t)}}. \quad (37)$$

If  $\epsilon = 1$  and  $\Theta < 0$  this is exactly of the form (36). Fig. 5.1 supports our finding in Theorem 11 and shows that Eq. (37) is chaotic for a wide range of  $\epsilon$ -values.

For  $\Theta > 0$  the family of maps (36) is not a full family of S-unimodal maps. However, computer simulations indicate that even in this case the Lyapunov exponent of (36) can be positive depending on the parameter values of  $\Theta, \mu$  and  $\epsilon$ . For positive values of  $\Theta$ , Eq. (36) can be used to model neural networks [9].

Another example of a full family of S-unimodal maps is given by the familiar logistic maps. In the next section we study in detail the emergent synchronous chaotic dynamics in networks of coupled logistic maps.

## 5.2 Coupled logistic maps

It is well-known that the logistic map

$$\ell_\rho(x) = \rho x(1-x), \quad \rho \in [0, 4] \text{ and } x \in [0, 1]$$

is a full family of S-unimodal maps. The logistic map is probably the best analyzed chaotic map; still not everything is understood rigorously. For convenience we briefly recall some properties. For  $\rho = 2$  the dynamics of the logistic map are very simple, with the fixed point  $x = 1/2$  attracting all points in the open interval  $(0, 1)$ . The logistic map

$\ell_\rho$  undergoes a period doubling route to chaos [17]. At  $\rho = 3$  the first period-doubling occurs, followed by further period-doubling bifurcations with increasing values of  $\rho$ , which accumulate at  $\rho \approx 3.57$ . For  $\rho > 3.57$  the logistic map can be chaotic but there are also so-called periodic windows in the parameter interval  $\rho \in (3.57, 4]$ . For  $\rho = 4$  it is maximally chaotic with a Lyapunov exponent  $\mu_{\ell_4} = \ln 2$ .

We consider a network of coupled logistic maps. Let  $f(x) = a_1x(1-x)$ ,  $\hat{g}(x) = a_2x(1-x)$  and

$$\epsilon = \frac{\rho - a_1}{a_2}. \quad (38)$$

Assume that  $a_1, a_2 \in (0, 4)$  and  $x(0) \in [0, 1]$ . Then the dynamics of the synchronized solution is given by

$$s(t+1) = \ell_\rho(s(t)) = \rho s(t)(1-s(t)). \quad (39)$$

For given  $a_1$  and  $a_2$  the coupling constant  $\epsilon$  can be used to control the dynamics of the synchronous solution, i.e.  $\epsilon$  can be used as bifurcation parameter. In particular, synchronous chaotic behavior can emerge in the whole network, even if the individual dynamics are very simple.

By an application of Corollary 10, the directly coupled network of logistic maps synchronizes if

$$\max_{k \geq 2} \log \left| 1 - \left( 1 - \frac{a_1}{\rho} \right) \lambda'_k \right| + \mu_{\ell_\rho} < 0. \quad (40)$$

For illustration we consider some concrete examples.

**Example 12.** Let  $f(x) = \hat{g}(x) = \ell_2(x)$ . Choosing  $\epsilon = 1$  yields  $\rho = 4$ , and the synchronous solution  $s(t) = \ell_4(t)$  becomes maximally chaotic. Thus, the whole network displays complicated dynamics although each unit of the network itself is dynamically simple.

Eq. (40) implies that the network synchronizes if all eigenvalues of the graph Laplacian (except  $\lambda'_1 = 0$ ) are contained in  $\mathcal{D}(2, 1)$ . Within the class of undirected graphs with nonnegative weights, the latter condition can only be satisfied for complete graphs [11]. However, for directed graphs or in the case of mixed signs there exist also non-complete graphs satisfying this condition [19].

In the next example we choose different functions  $f$  and  $\hat{g}$  that lead to the same synchronous solution. Interestingly, the condition on the eigenvalues is this time different than in the case of Example 12.

**Example 13.** Let  $f(x) = \ell_1(x)$  and  $\hat{g} = \ell_3(x)$ . Choosing  $\epsilon = 1$  implies that the synchronous solution is the same as in Example 12, i.e.  $s(t) = \ell_4(x)$ .

The network synchronizes if all eigenvalues (except  $\lambda'_1 = 0$ ) of the graph Laplacian are contained in  $\mathcal{D}(\frac{4}{3}, \frac{2}{3})$ . In contrast to Example 12, there also exists non-complete undirected graphs with positive weights that satisfy the latter condition.

Comparing Example 12 and Example 13 shows one interesting point. In both Examples the synchronous solution  $s(t)$  and the overall coupling strengths are identical. However, in Example 12 the network synchronizes if all eigenvalues are contained in  $\mathcal{D}(2, 1)$  whereas the same is true for Example 13 if all eigenvalues are contained in  $\mathcal{D}(\frac{4}{3}, \frac{2}{3})$ . Thus, in contrast to diffusively coupled units, the synchronizability of a directly coupled network is not completely determined by the synchronous solution  $s(t)$ , the overall coupling strength  $\epsilon$  and the network topology (i.e. the eigenvalues of the coupling matrix), but depends also on the special choices of  $f$  and  $\hat{g}$ . Clearly, this can already be seen from the definition of  $\chi_k^{\text{direct}}$ .

## 6 Suppression of chaos

Besides the emergence of chaos in a network of simple units, the opposite is also possible. In this section we show that non-diffusive coupling can also be used to suppress chaos. Chaos suppression in single systems is a well-established field; for an overview see [20] and the references therein. In our setting, suppression arises in networks through synchronization of the states of the units.

As a first example, we consider a network of directly coupled chaotic logistic maps.

**Example 14.** Let  $f(x) = \hat{g}(x) = \ell_4(x)$  be given and choose  $\epsilon = (\frac{2.1}{4} - 1)$ . This choice implies that the synchronous behavior is given by  $s(t) = \ell_{2.1}(t)$  and is non-chaotic. Corollary 10 implies that the network synchronizes if all eigenvalues of the graph Laplacian are contained in  $\mathcal{D}(-1.11, 10.99)$ .

Example 14 shows that the network synchronizes for a wide range of eigenvalues  $\lambda'_k$ . Compared to synchronous chaotic behavior, studied in Example 12 and 13, the radius of the disk  $\mathcal{D}$  is much larger for simple synchronous behavior. The reason can be seen from condition (35): A smaller Lyapunov exponent for the synchronous behavior implies less restrictions on the allowable values of  $\lambda'_k$ .

Lemma 1 implies that all eigenvalues of  $\mathcal{L}$  are contained in the disk  $\mathcal{D}(1, r)$ . For sufficiently small  $r$  the latter disk is contained in  $\mathcal{D}(-1.11, 10.99)$ . So, instead of calculating all eigenvalues of the coupling matrix, the knowledge of the radius  $r$  can be sufficient to determine whether the network synchronizes. Hence, the quantity  $r$  already gives some insights concerning the robustness of the synchronous state.

Motivated by the above example, we will give in the next section sufficient conditions for synchronization in terms of  $r$ . In fact, these conditions will not depend on the eigenvalues of the coupling matrix. Again, we want to point out that this is only possible if the synchronous behavior is not chaotic.

### 6.1 Direct coupling

We restrict ourselves to the case of direct coupling where  $\hat{g}(x) = bf(x)$ . It follows from Corollary 10 and Lemma 1 that the network synchronizes if

$$\mu_{(1+\epsilon b)f} < \log \left| \frac{1 + \epsilon b}{1 + |\epsilon b|r} \right|. \quad (41)$$

Again, we see that a simpler synchronous behavior in the sense of a smaller Lyapunov exponent implies that the network synchronizes for a large class of network topologies.

**Example 15.** Let  $f(x) = \hat{g}(x) = \ell_4(x)$  and choose  $\epsilon = (\frac{\rho}{4} - 1)$ . This choice implies that  $s(t) = \ell_\rho(t)$ . By Eq. (41), the network synchronizes if

$$\mu_{\ell_\rho} + \log \left| \frac{4}{\rho} + \left( \frac{4}{\rho} - 1 \right) r \right| < 0. \quad (42)$$

The left-hand-side of (42) is plotted in Figure 2.

- For  $\rho = 2$ ,  $x^* = 1/2$  is an attracting fixed point of  $s(t) = \ell_2(t)$  that attracts all points in the open interval  $(0, 1)$ . For  $x(t=0) = x_0 \in (0, 1)$  we have

$$x(t) = 1/2[1 - (1 - 2x_0)^{2^t}].$$



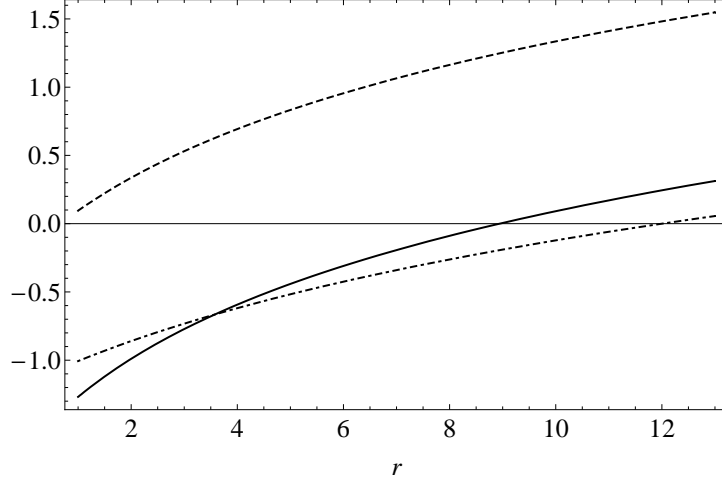


Figure 2: Plot of  $\mu_{\ell_\rho} + \log \left| \frac{4}{\rho} + \left( \frac{4}{\rho} - 1 \right) r \right|$  as a function of  $r$ . The dot-dashed line corresponds to the parameter value  $\rho = 3.25$ , the dashed line to  $\rho = 2.5$  and the solid line to  $\rho = 2.1$ .

Because of this fast convergence to  $\frac{1}{2}$ , the fact that  $\ell'_2(\frac{1}{2}) = 0$  implies that  $\mu_{\ell_2} = -\infty$ .<sup>5</sup> Thus the network synchronizes for all network topologies.

- For  $\rho = 2.1$  and  $\rho = 3.25$  the solid and dot-dashed line in Fig. 2 show that the network synchronizes for all network topologies that satisfy  $r < 8$  or  $r < 12$  respectively. In comparison to Example 14 here we only use the information given by  $r$  instead of using all eigenvalues of the coupling matrix.
- For  $\rho = 2.5$  the dashed line in Fig. 2 shows that the function  $\mu_{\ell_{2.5}} + \log \left| \frac{4}{2.5} + \left( \frac{4}{2.5} - 1 \right) r \right|$  is never negative. Hence estimates based on  $r$  are too crude to obtain synchronization information, however in such a case we can use Corollary 10 to conclude that the network synchronizes if all eigenvalues  $\lambda'_k$  of  $\mathcal{L}$  (except  $\lambda'_1 = 0$ ) are contained in a disk centered at  $-5/3$  with a radius  $10/3$ .

Finally, we give an example of synchronization independent of network topology when all the weights have the same sign.

**Example 16.** Let  $\hat{g}(x) = bf(x)$  be arbitrarily maps. Assume that all weights in the network are either nonnegative or nonpositive, i.e.  $r = 1$ . If  $\epsilon b \geq 0$  then condition (41) is satisfied if

$$\mu_{((1+\epsilon b)f)} < \log 1 = 0.$$

If  $\epsilon b < 0$  then condition (41) is satisfied if

$$\mu_{((1+\epsilon b)f)} < \log \left| \frac{1 + \epsilon b}{1 - \epsilon b} \right|.$$

<sup>5</sup>Because of this property, some authors call the fixed point  $\frac{1}{2}$  superstable. [21].

## 7 Conclusion and discussion

In this work we studied complete synchronization in coupled map networks of identical units. We have generalized synchronization analysis to directed networks with both positive and negative weights and general pairwise coupling functions. This generalization is especially important for analyzing real-world networks. For example, in neural networks the coupling function is non-diffusive. Excitation and inhibition are modeled by positive and negative weights, respectively, and only the pre-synaptic neuron influences the post-synaptic one but not vice versa. Thus, directed networks with signed weights are needed to model neural networks in an appropriate way.

We have derived sufficient conditions for local synchronization, which are expressed in terms of the maximal mixed transverse exponent. We have shown that, in contrast to diffusively coupled units, non-diffusively coupled networks can display new synchronized behavior that the individual unit is not able to show. The new synchronous behavior is influenced by the overall coupling strength that plays the role of a bifurcation parameter. Again, this is important in neural networks. Changing the coupling strength in a learning process allows the network to learn new, possibly much richer behavior than before. In particular, synchronized chaotic behavior can arise in networks of non-chaotic units with non-chaotic interactions functions. Conversely, chaos can be suppressed through synchronization in networks of chaotic units. This may have practical implications in the field of chaos control. Often chaos is controlled by applying time-delayed external feedback. In our approach chaos can be controlled by changing an internal parameter of the system.

There exists natural extensions of this work. One direction is to generalize the synchronization analysis to networks of non-identical units. Here the problem is more challenging, since complete synchronization is usually not possible, and one must look for other suitable types of solutions and investigate their stability. Other directions for extension include higher-dimensional and/or continuous-time systems. In all cases, the possibility of the emergence of new dynamics via synchronization offers a helpful perspective in our efforts to understand complex systems.

## A Definition of a full family of S-unimodal maps

**Definition 17** (Unimodal Map). *Let  $f : I = [0, 1] \rightarrow I = [0, 1]$ . The map is unimodal if*

1.  $f(0) = f(1) = 0$
2.  $f$  has a unique critical point  $c$  (i.e.  $f'(c) = 0$ ) with  $0 < c < 1$ .

**Definition 18** (Schwarzian Derivative). *The Schwarzian derivative of a function  $f$  at  $x$  is*

$$Sf(x) = \frac{f'''(x)}{f'(x)} - \frac{3}{2} \left( \frac{f''(x)}{f'(x)} \right)^2.$$

The important role of a negative Schwarzian derivative was discovered by Singer [22]. A negative Schwarzian derivative restricts the number of stable periodic orbits. Singer showed that a unimodal map whose Schwarzian derivative is negative has at most one stable periodic orbit. Furthermore, if the critical point is not attracted to a stable periodic orbit then the map has no stable orbit at all.

**Definition 19** (Itinerary). *Let  $x \in I$ . The itinerary of  $x$  under  $f$  is the infinite sequence  $S(x) = (s_0 s_1 s_2, \dots)$  where*

$$s_j = \begin{cases} 0 & \text{if } f^j(x) < c \\ 1 & \text{if } f^j(x) > c \\ C & \text{if } f^j(x) = c. \end{cases}$$

The idea of kneading sequences goes back to Milnor and Thurston [23].

**Definition 20** (Kneading Sequence). *The kneading sequence  $K(f)$  of  $f(x)$  is the itinerary of  $f(c)$ , i.e.,  $K(f) = S(f(c))$ .*

**Definition 21** (Full family of S-unimodal maps). *Let  $f_\mu$  be a family of unimodal maps with  $\mu_0 \leq \mu \leq \mu_1$ .  $f_\mu$  is called a full family of S-unimodal maps if*

1.  $f_{\mu_0}(x) \equiv 0$  for all  $x \in I$ .
2. When  $\mu = \mu_1$ ,  $K(f_\mu) = (100\bar{0}\dots)$ .
3.  $Sf_\mu(x) < 0$  for all  $\mu > \mu_0$  and  $x \in I$ .

## B Proof of Theorem 11

*Proof.* It is straightforward to show that  $f_\mu$  is unimodal for all  $\mu$ . The first two points in Definition 21 obviously hold because  $f_{\mu_1}^2(c) = 0$  and 0 is a fixed point. So we only have to prove that  $Sf_\mu(x) < 0$  for all  $\mu > \mu_0 = 0$ . We calculate the following derivatives.

$$\begin{aligned} f'_\mu(x) &= \frac{1 - e^{-\mu}}{1 + e^{-\mu}} \Theta - \frac{2\mu\Theta e^{-\mu x}}{(1 + e^{-\mu x})^2} \\ f''_\mu(x) &= 2\mu^2\Theta e^{-\mu x} \left[ \frac{1}{(1 + e^{-\mu x})^2} - \frac{2e^{-\mu x}}{(1 + e^{-\mu x})^3} \right] \\ f'''_\mu(x) &= 2\mu^3\Theta e^{-\mu x} \left[ -\frac{1}{(1 + e^{-\mu x})^2} + \frac{6e^{-\mu x}}{(1 + e^{-\mu x})^3} - \frac{6e^{-2\mu x}}{(1 + e^{-\mu x})^4} \right]. \end{aligned}$$

Putting  $a := \frac{1 - e^{-\mu}}{1 + e^{-\mu}}$  and  $b := a(1 + e^{-\mu x})^2 - 2\mu e^{-\mu x}$ , we have:

$$\begin{aligned} \frac{f'''_\mu(x)}{f'_\mu(x)} &= \frac{\frac{1}{b^2} [-2a\mu^3 e^{-\mu x} (1 + e^{-\mu x})^2 + 4\mu^4 e^{-2\mu x} + 12a\mu^3 e^{-2\mu x} (1 + e^{-\mu x})]}{-\frac{24\mu^4 e^{-3\mu x}}{1 + e^{-\mu x}} - 12a\mu^3 e^{-3\mu x} + \frac{24\mu^4 e^{-4\mu x}}{(1 + e^{-\mu x})^2}} \\ -\frac{3}{2} \left( \frac{f''_\mu(x)}{f'_\mu(x)} \right)^2 &= \frac{1}{b^2} \left[ -6\mu^4 e^{-2\mu x} + \frac{24\mu^4 e^{-3\mu x}}{1 + e^{-\mu x}} - \frac{24\mu^4 e^{-4\mu x}}{(1 + e^{-\mu x})^2} \right] \end{aligned}$$

Thus, the Schwarzian derivative

$$\begin{aligned} Sf_\mu(x) &= \frac{f'''_\mu(x)}{f'_\mu(x)} - \frac{3}{2} \left( \frac{f''_\mu(x)}{f'_\mu(x)} \right)^2 \\ &= \underbrace{\frac{-2a\mu^3 e^{-\mu x}}{b^2}}_{<0} \underbrace{\left[ 1 + e^{-2\mu x} + \left( \frac{\mu}{a} - 4 \right) e^{-\mu x} \right]}_{=: g_\mu(x)} \end{aligned}$$

is negative if  $g_\mu(x) > 0$ . The critical point of  $g_\mu(x)$  is given by

$$c = \frac{\ln\left(2 - \frac{\mu}{2a}\right)}{-\mu}.$$

It is easy to verify that this critical point  $c$  is actually a minimum of the function  $g_\mu(x)$ . First, we assume that  $c \in (0, 1)$ . This leads to

$$e^{-\mu} < 2 - \frac{\mu}{2a} < 1. \quad (43)$$

Inserting the critical point yields:

$$\begin{aligned} g_\mu(c) &= 1 + \left(2 - \frac{\mu}{2a}\right)^2 + \left(\frac{\mu}{a} - 4\right) \left(2 - \frac{\mu}{2a}\right) \\ &= -3 + 2\frac{\mu}{a} - \left(\frac{\mu}{2a}\right)^2 \\ &= 1 - \underbrace{\left(2 - \frac{\mu}{2a}\right)^2}_{<1} > 0 \end{aligned}$$

So we only have to check that  $g_\mu(x) > 0$  at the boundary. First we consider the case  $x = 0$ .

$$g_\mu(0) = -2 + \frac{\mu}{a} = -2 + \frac{1 + e^{-\mu}}{1 - e^{-\mu}}\mu$$

Calculating the minimum of  $g_\mu(0)$  with respect to  $\mu$  yields:

$$\begin{aligned} \frac{dg_\mu(0)}{d\mu} &= \frac{1 + (1 - \mu)e^{-\mu}}{1 - e^{-\mu}} - \frac{\mu e^{-\mu}(1 + e^{-\mu})}{(1 - e^{-\mu})^2} \stackrel{!}{=} 0 \\ \Rightarrow 1 - 2\mu e^{-\mu} - e^{-2\mu} &= 0 \end{aligned}$$

Hence, we see that  $\mu = 0$  is the minimum. Using l'Hospital's rule we obtain:

$$\lim_{\mu \searrow 0} g_\mu(0) = -2 + \lim_{\mu \searrow 0} \frac{\mu(1 + e^{-\mu})}{1 - e^{-\mu}} = -2 + \lim_{\mu \searrow 0} \frac{1 + e^{-\mu} - \mu e^{-\mu}}{e^{-\mu}} \searrow 0$$

This shows that  $g(0) > 0$  if  $\mu > 0$ . The case  $x = 1$  is treated in the same way. Thus the family (36) is a full family of S-unimodal maps.  $\square$

## References

- [1] A. Arenas, A. Diaz-Guilera, J. Kurths, Y. Moreno, and C. Zhou. Synchronization in complex networks. *Physics Reports*, 469:93–153, 2008.
- [2] M. Chavez, D. Hwang, and S. Boccaletti. Synchronization processes in complex systems. *Eur. Phys. J. Special Topics*, 146:129–144, 2007.
- [3] A. Pikovsky, M. Rosenblum, and J. Kurths. *Synchronization: A universal concept in nonlinear sciences*. Cambridge University Press, Cambridge, 2001.

- [4] K. Kaneko. Period-doubling of kink-antikink patterns, quasi-periodicity in antiferro-like structures and spatial intermittency in coupled map lattice- toward a prelude to a field theory of chaos. *Prog. Theoret. Phys.*, 72:480–486, 1984.
- [5] J. Jost and M. Joy. Spectral properties and synchronization in coupled map lattices. *Physical Review E*, 65(016201), 2001.
- [6] W. Lu and T. Chen. Synchronization analysis of linearly coupled networks of discrete time systems. *Physica D*, 198:148–168, 2004.
- [7] F. M. Atay and Ö. Karabacak. Stability of coupled map networks with delays. *SIAM J. Applied Dynamical Systems*, 5(3):508–527, 2006.
- [8] F. M. Atay, J. Jost, and A. Wende. Delays, connection topology, and synchronization of coupled chaotic maps. *Physical Review Letters*, 92:144101, 2004.
- [9] F. Bauer, F. M. Atay, and J. Jost. Synchronized chaos in networks of simple units. submitted.
- [10] F. Bauer. Spectral properties of the normalized graph laplace operator of directed graphs. in preparation.
- [11] F. R. K. Chung. *Spectral Graph Theory*, volume 92 of *CBMS*. American Mathematical Society, 1997.
- [12] Roger A. Horn and Charles R. Johnson. *Matrix Analysis*. Cambridge University Press, 2006.
- [13] Richard A. Brualdi and Herbert J. Ryser. *Combinatorial Matrix Theory*. Cambridge University Press, 1991.
- [14] W. Lu, F. M. Atay, and J. Jost. Synchronization of discrete-time dynamical networks with time-varying couplings. *SIAM J. Math. Anal.*, 39(4):1231–1259, 2007.
- [15] K. Kaneko, editor. *Theory and applications of coupled map lattices*. Wiley, New York, 1993.
- [16] D. G. Aronson and N. Kopell. Amplitude response of coupled oscillators. *Physica D*, 41:403–449, 1990.
- [17] R. Devaney. *An introduction to chaotic dynamical systems - second edition*. Addison Wesley, 1989.
- [18] D. Whitley. Discrete dynamical systems in dimensions one and two. *Bull. London Math. Soc.*, 15:177–217, 1983.
- [19] F. Atay and F. Bauer. Synchronizability of coupled oscillators in directed and signed networks. *in preparation*.
- [20] E. Schöll and H.G. Schuster. *Handbook of chaos control, 2nd edition*. Wiley-Vch, 2007.
- [21] Jan Froyland. *Introduction to chaos and coherence*. IOP Publishing, 1992.

- [22] D. Singer. Stable orbits and bifurcations of maps of the interval. *SIAM. J. Appl. Math.*, 35:260–267, 1978.
- [23] J. Milnor and W. Thurston. On iterated maps of the interval i & ii. *Princeton preprints*, 1977.